

Thin magnetic wires for GMI applications

A. ZHUKOV^{a,b*}, M. IPATOV^a, V. ZHUKOVA^a

^a*Dpto. de Fis. Mater., UPV/EHU San Sebastián 20009, Spain*

^b*IKERBASQUE, Basque Foundation for Science, 48011 Bilbao, Spain*

Magnetically soft thin amorphous microwires attracted recently great attention because of their excellent soft magnetic properties and giant magneto-impedance (GMI) effect, thin dimensions and possibility for applications in magnetic micro-sensors. We overview results on development of magnetically soft microwires with high GMI effect and report last results on studies of GMI (diagonal and off-diagonal components) at high frequencies (up to 4 GHz) and correlation of observed GMI effect with soft magnetic behaviour of thin Co-Fe-rich amorphous microwires (metallic diameter between 3 and 20 μm) and on optimization of GMI effect. We observed and analyzed low-field hysteresis of GMI effect and its dependence on circular dc bias magnetic field and discuss the nature the low-field hysteresis in terms of helical magnetic anisotropy and the effect of the bias field. Choosing samples composition, annealing conditions and geometry we were able to tailor their magnetoelastic anisotropy and respectively magnetic softness and GMI.

(Received January 31, 2012; accepted April 11, 2012)

Keywords: Glass-coated microwires, GMI effect, Magnetoelastic anisotropy

1. Introduction

Recently studies of soft magnetic properties and giant magneto-impedance (GMI) effect of thin amorphous glass coated microwires attracted considerable interest mainly owing to possibilities of use of such wires for sensitive magnetic field microsensors [1-3]. The GMI effect is understood as a giant change of the impedance of a magnetically soft conductor upon the application of external magnetic field [4,5]. Main advantages of this method of magnetic field detection are small-size, high-performance and low-cost of GMI sensors. As a result of intensive studies of the GMI effect in the past decade, the magnetic field detection resolution as high as 1 μOe has been achieved [6] and the first low-cost multi-axis sensors in microchip with claimed nano-Tesla sensitivity that can operate over a wide temperature range have recently appeared on the market [7].

It is worth mentioning, that most of previously reported results correspond to the microwires with the diameter above 20 μm . Consequently last challenge for industrial application is related with miniaturization of MI elements and consequently considerable efforts have been paid to development of thin magnetically soft microwires with high GMI effect [3,8].

As previously reported elsewhere [2,3] the hysteretic magnetic properties of glass-coated microwires are rather different from those of conventional amorphous wires mostly because of additional magnetoelastic energy related with strong internal stresses induced during the rapid solidification of the thin wire surrounded by the glass coating when using Taylor-Ulitovsky method [2,3,9]. Recently certain progress has been achieved in enhancement of magnetic softness and GMI effect of glass coated microwires, paying most attention on alloy composition and post-fabrication processing of microwires

aiming improvement of the magnetic permeability and GMI effect through the diminishing of the magnetoelastic anisotropy related with strong internal stresses and induction of desirable magnetic anisotropy. Consequently, adequate choosing of the geometric parameters determined by the fabrication procedure and conditions of heat treatment can significantly enhance soft magnetic properties and GMI effect (up to 600%) [2, 3, 8, 9].

In most of applications a high linearity of MI dependence and low hysteresis are desirable. Anti-symmetrical MI curve with linear region has been obtained in current pulsed excitation scheme of wires using detection of off-diagonal GMI component [3,10]. At the same time we have recently showed, that linearity and shape of off-diagonal component in microwires can be tailored by thermal treatment [8]. Additionally, considerable GMI hysteresis has been observed and analyzed in microwires possessing helical anisotropy [11].

In this paper we analyze the results on GMI effect in thin microwires paying special attention to tailoring the GMI effect of thin glass-coated amorphous microwires by choosing the sample geometry (ratio, ρ , between metallic nucleus diameter, d and the total microwire diameter, D) and annealing parameters with the aim to improve magnetic field and stress sensitivity of the GMI effect and diminish the GMI hysteresis.

2. MI in microwires at high frequencies

Further, we will consider a simple model of MI at high frequency in amorphous microwire that however, qualitatively agrees with the experimental results. For wire geometry and the high-frequency approximation (strong skin effect) the longitudinal Z_{zz} and off-diagonal $Z_{\varphi z}$ impedance components can be expressed as [13]:

$$Z_{zz} = (1-i)(\sqrt{\tilde{\mu}+1} \sin^2 \varphi + \cos^2 \varphi) R_{dc} \frac{a}{\delta_0}, \quad (1)$$

$$Z_{\varphi z} = (1-i)(\sqrt{\tilde{\mu}+1} - 1) \sin \varphi \cos \varphi, \quad (2)$$

where φ is the angle between the magnetization and the transversal plane, R_{dc} is the wire dc resistance, a is the wire radius, $\delta_0 = (2\rho/\mu_0\omega)^{1/2}$ is the nonmagnetic skin depths, ω is the angular frequency, and $\tilde{\mu}$ is the effective transverse permeability [11].

The longitudinal Z_{zz} and off-diagonal $Z_{\varphi z}$ impedances can be very sensitive to external axial magnetic field H_E in a wire that exhibits a high sensitivity of angle φ on H_E . Supposing that the surface layer, where the high frequency current is concentrating, is in a mono-domain state (see discussion in [14]), then under the effect of axial external magnetic field H_E and dc bias field H_B created by bias current I_B , the equilibrium angle φ_0 , can be determined from the equation of energy minimization [11]:

$$\frac{1}{2} H_k \sin 2(\varphi_0 + \alpha) - H_E \cos \varphi_0 + H_B \sin \varphi_0, \quad (3)$$

where H_k is the surface anisotropy field and α is the angle between the anisotropy easy axis and the transversal plane. We neglect the demagnetizing fields and the contribution of the exchange energy.

From Eq. (3), that is actually the well known Stoner–Wohlfarth model, the equilibrium angle φ_0 can be found. As one can see, the equilibrium φ_0 , and consequentially the MI dependences, depend on external magnetic field H_E , circumferential bias field H_B , anisotropy field H_k , and anisotropy angle α . Further we consider the effect of these parameters (bias field H_B , anisotropy field H_k , and anisotropy angle α) on the impedance dependence on external magnetic field H_E .

3. Tailoring of magnetic properties and GMI effect in thin glass-coated microwires

3.1. Effect of microwire geometry

As mentioned above, the strength of the internal stresses, σ , is related with simultaneous solidification of metallic nucleus inside glass coating and most important contribution is induced by the difference in the thermal expansion coefficients of metallic nucleus and outer glass coating solidifying simultaneously [2, 3, 15-17]. Consequently, ρ -ratio defined as the ratio between metallic nucleus diameter, d , and total microwires diameter, D , affects the strength of internal stresses. The effect of the ρ ratio on the hysteresis loops of nearly-zero magnetostrictive $\text{Co}_{67}\text{Fe}_{3.85}\text{Ni}_{1.45}\text{B}_{11.5}\text{Si}_{14.5}\text{Mo}_{1.7}$ microwires is shown in Fig.1. All studied samples

exhibited inclined almost unhysteretic M(H) loops with extremely low coercivities (up to 4 A/m). It is remarkable that the samples with rather different metallic nucleus diameter but with the same ρ -ratio have almost the same hysteresis loops (see hysteresis loops of the samples with $\rho=0,64$ and different d). Magnetic anisotropy field, H_k , is found to be determined by the ρ -ratio, increasing with ρ .

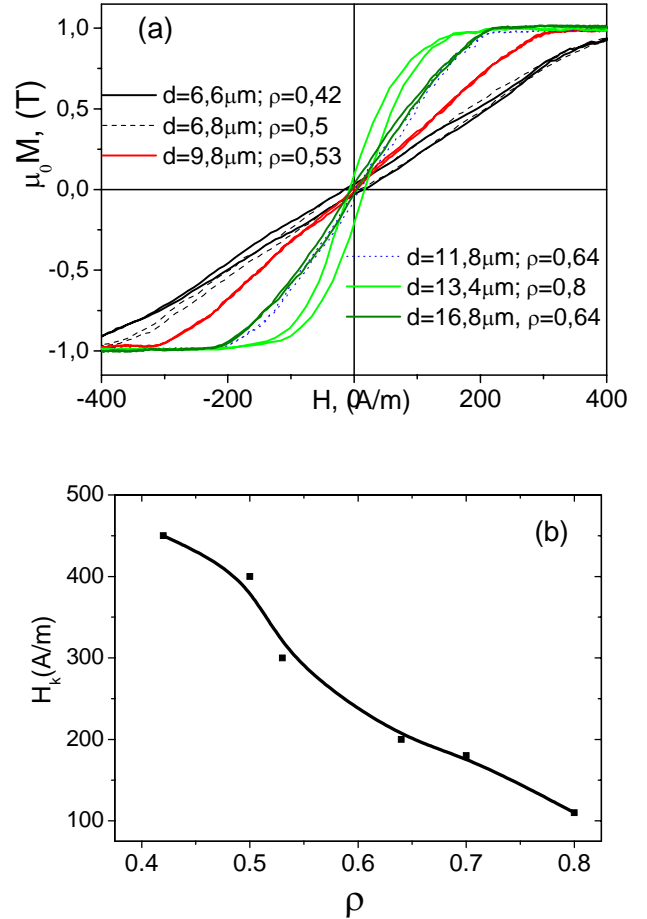


Fig. 1. Hysteresis loops of $\text{Co}_{67.1}\text{Fe}_{3.8}\text{Ni}_{1.4}\text{Si}_{14.5}\text{B}_{11.5}\text{Mo}_{1.7}$ microwires with different geometry (a) and dependence of H_k on ρ -ratio (b).

Such $H_k(\rho)$ dependence has been attributed to the magnetoelastic energy contribution given by

$$K_{me} \approx 3/2 \lambda_s \sigma_i, \quad (4)$$

where λ_s is the saturation magnetostriction and σ_i is the internal stress. The magnetostriction constant is mostly determined by the chemical composition and achieves almost nearly-zero values in amorphous alloys based on Fe-Co with $\text{Co/Fe} \approx 70/5$ $\lambda_s \approx 0$ [2, 17]. On the other hand, the estimated values of the internal stresses in these glass coated microwires arising from the difference in the thermal expansion coefficients of metallic nucleus and glass coating are of the order of 100-1000 MPa, depending strongly on the ratio between the glass coating thickness

and metallic core diameter [2-4, 12,15], increasing with decreasing ρ -ratio. Considering elevated internal stresses stress dependence of magnetostriction constant should be taken into account as well [2, 18]:

$$\lambda_s = (\mu_0 M_s / 3)(dH_k / d\sigma), \quad (5)$$

where $\mu_0 M_s$ is the saturation magnetization.

Considering abovementioned we should assume that any method allowing change the internal stresses (by using thermal treatment, chemical etching, controlling microwire geometry) can change drastically magnetic anisotropy and consequently the hysteresis loops and the GMI behavior of glass coated microwires.

3.2. Tailoring of magnetic properties by heat treatment and induced magnetic anisotropy

Heat treatment resulting in structural and stress relaxation in amorphous alloys is a commonly used method for tailoring the magnetoelastic energy [2]. In the case if the alloy composition contains more than one transition metal the pair ordering mechanism of induced magnetic anisotropy especially if magnetic field and/or stress is applied during the heat treatment should be also taken into account [2, 18].

Effect of current annealing (CA) and magnetic field current annealing (FCA) on hysteresis loop of $\text{Co}_{67}\text{Fe}_{3.85}\text{Ni}_{1.45}\text{B}_{11.5}\text{Si}_{14.5}\text{Mo}_{1.7}$ is shown in Fig.2. Axial magnetic field during FCA (about 8000A/m) has been much higher than circular magnetic field created by the current. As can be appreciated from comparison of Figs 2a and 2b, application of magnetic field during annealing results in induction of axial magnetic anisotropy.

Application of stress during stress annealing of $\text{Fe}_{74}\text{B}_{13}\text{Si}_{11}\text{C}_2$ microwires resulted in induction of considerable stress induced anisotropy [19]. In this case rectangular hysteresis loop associated with the strong axial magnetic anisotropy induced by residual stresses of mostly tensile origin after stress annealing converted into inclined hysteresis loop with large enough magnetic anisotropy field (Fig.3a)[17]. In fact the hysteresis loops can be tailored varying the time or temperature of stress annealing and consequently a variety of hysteresis loop with different magnetic anisotropy can be obtained in $\text{Fe}_{74}\text{B}_{13}\text{Si}_{11}\text{C}_2$ microwires, as can be observed in Fig.3a.

Such behavior should be attributed to the compressive stresses induced by the SA in presence of tensile stress, compensating axial stresses induced during microwires fabrication involving simultaneous solidification of the metal and glass.

The strength of such compressive stresses depends on both time and temperature of annealing.

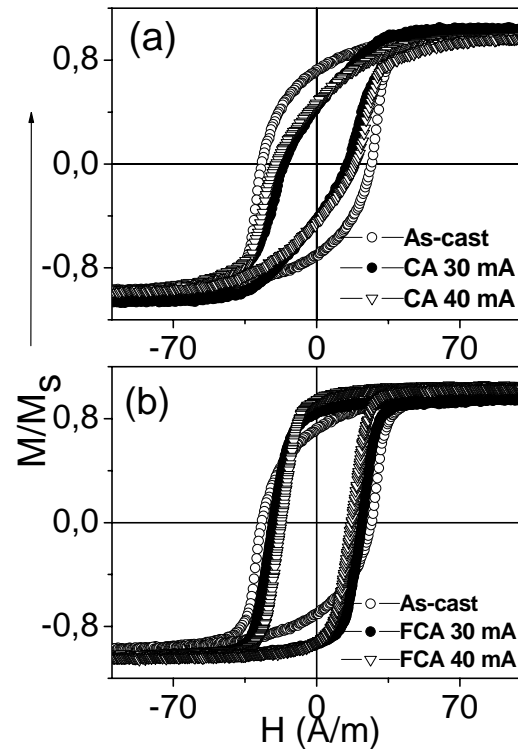


Fig. 2. Effect of CA (a) and FCA (b) treatments on bulk hysteresis loops of $\text{Co}_{67}\text{Fe}_{3.85}\text{Ni}_{1.45}\text{B}_{11.5}\text{Si}_{14.5}\text{Mo}_{1.7}$ microwires ($d=22.4 \mu\text{m}$, $D=22.8 \mu\text{m}$).

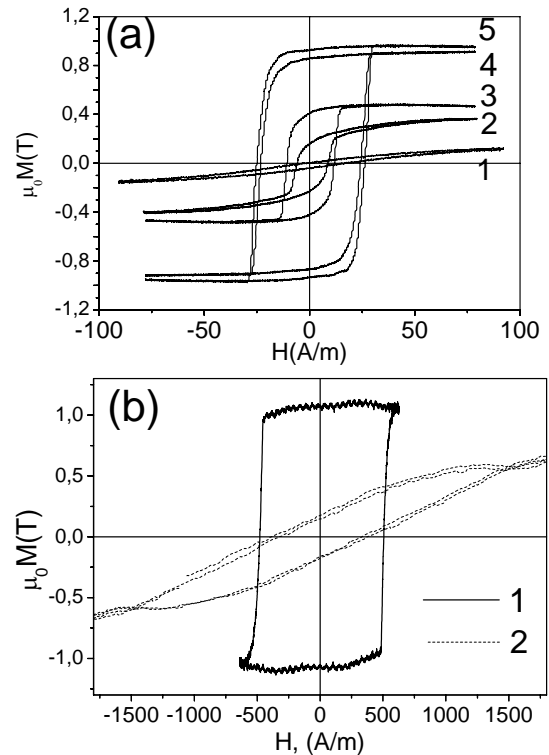


Fig. 3. Hysteresis loops of $\text{Fe}_{74}\text{B}_{13}\text{Si}_{11}\text{C}_2$ microwire annealed under applied stress of 500 MPa (a) at (1) – 300 °C 3 hours, (2) – 280 °C 40 min, (3)– 265 °C 40 min, (4) 235 °C 40 min and (5)– 215 °C 40 min and (b) stress induced changes of hysteresis loops of the same microwires (1- measured under applied stress, 2- measured without stress).

Under applied stress, the hysteresis loop changes drastically, exhibiting enhanced stress sensitivity (Fig.3b).

Another relevant effect related with stress sensitivity of hysteresis loop induced by annealing under stress is the stress-impedance (SI) effect, i.e. impedance change under applied stress observed in samples with induced stress anisotropy (see Fig.4)

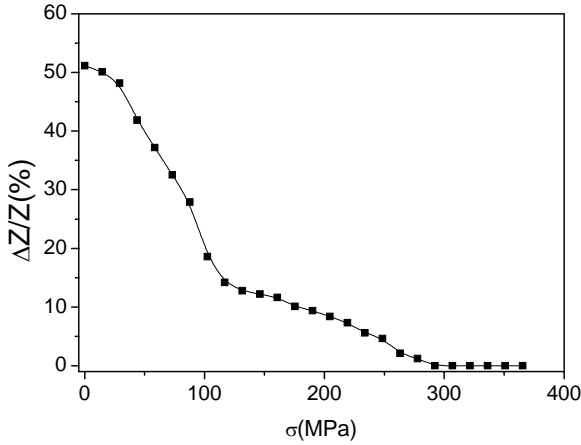


Fig. 4. Stress impedance effect of stress annealed $Fe_{7.4}B_{1.3}Si_{11}C_2$ glass-coated microwire under stress (468 MPa) at $275^\circ C$ for 0.5h measured at frequency, $f=10$ MHz for the driving current amplitude of 2 mA

It is worth mentioning, that the SI effect does not require application of magnetic field and it can be used for stress and vibration detection.

3.3. Tailoring of the GMI effect (including off-diagonal component)

Like in the case of hysteresis loops the sample geometry strongly affects the GMI effect, i.e. magnetic field dependences of impedance (Fig.5). Here we present magnetic field, H , dependence of real part, Z' of the longitudinal wire impedance Z ($Z = Z' + iZ''$). Indeed we observe (see Fig.5) that the sample geometry strongly affects the DC axial magnetic field dependence of the real part of GMI, Z' of $Co_{67}Fe_{3.85}Ni_{1.45}B_{11.5}Si_{14.5}Mo_{1.7}$ microwires measured at different frequencies f .

Such considerations regarding dependence of the GMI response on the samples geometry should be taken into account for development of extremely thin microwires. It is important for microminiaturized sensor application since the demagnetizing factor starts to affect the domain structure and magnetic properties when geometric ratio of microwire diameter to its longitude becomes lower [20]. It should be assumed that the internal stresses relaxation after heat treatment should drastically change both the soft magnetic behavior and $\Delta Z/Z(H)$ dependence mostly because of the stress dependence of the magnetostriction described in ref [18]:

$$\lambda_s(\sigma) = \lambda_s(0) - A\sigma \quad (6)$$

where $\lambda_s(0)$ is the saturation magnetostriction constant without applied stresses and A is the positive coefficient of the order of 10^{-10} MPa.

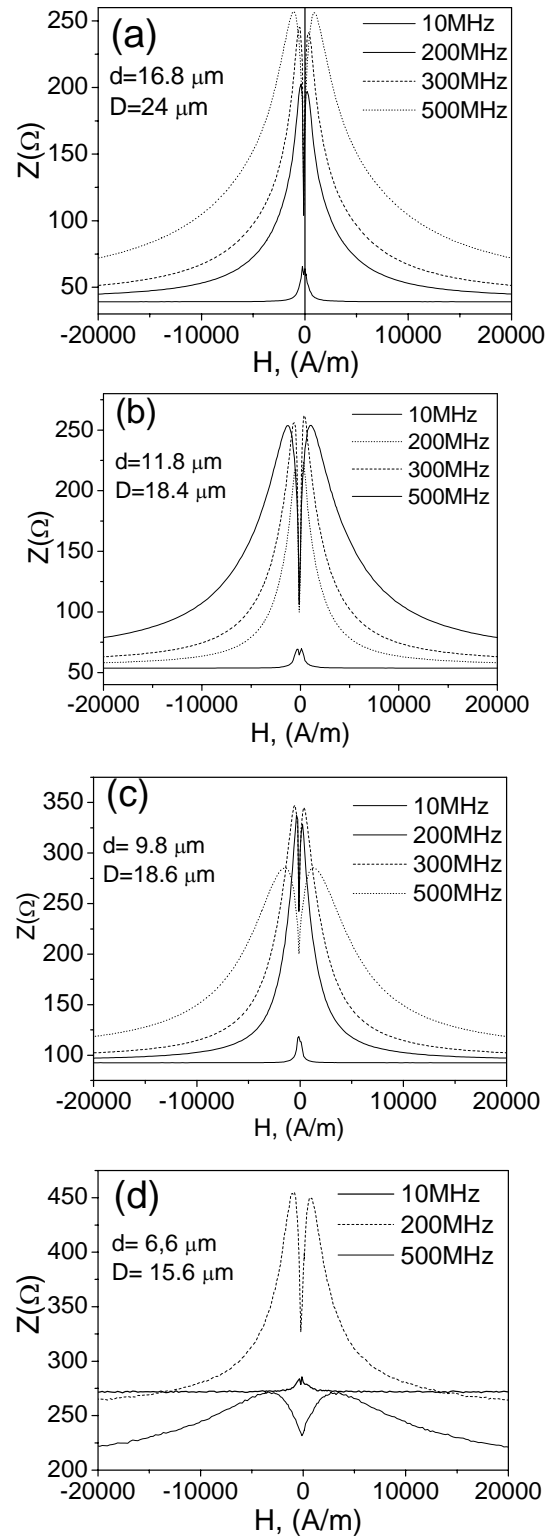


Fig. 5. $Z(H)$ dependence $Co_{67}Fe_{3.85}Ni_{1.45}B_{11.5}Si_{14.5}Mo_{1.7}$ microwires with different geometry measured at frequencies $f=10, 200$ and 500 MHz

In fact one should take into account that both magnetic permeability as well as magneto-impedance have tensor character. The off-diagonal components measured using pulsed excitation possess the asymmetrical dependence on magnetic field, that is a necessary condition for determination the magnetic field direction [10,11]. It is worth mentioning, that for practical sensors the pulsed excitation is preferred over a sinusoidal one because of the simple electronic design and low power consumption. The practical circuit design [10, 21] consists of a pulse generator, sensor element and output stage.

The sharp pulses are produced by passing squared wave pulses through the differential circuit Figs. 6,7 show field dependence of the off-diagonal voltage response, V_{out} measured using pulsed scheme as described elsewhere [7-9] in $\text{Co}_{67.1}\text{Fe}_{3.8}\text{Ni}_{1.4}\text{Si}_{14.5}\text{B}_{11.5}\text{Mo}_{1.7}$ ($\lambda_s \approx 3 \cdot 10^{-7}$) microwire with different geometry: metallic nucleus diameter and total diameter with glass coating are 6.0/10.2, 7.0/11.0 and 8.2/13.7 μm .

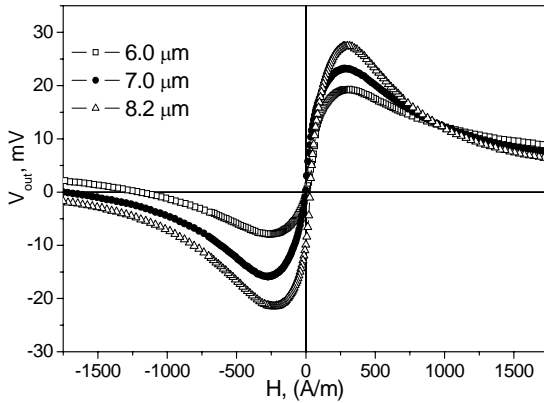


Fig. 6. $V_{out}(H)$ response of $\text{Co}_{67.1}\text{Fe}_{3.8}\text{Ni}_{1.4}\text{Si}_{14.5}\text{B}_{11.5}\text{Mo}_{1.7}$ microwires with different d .

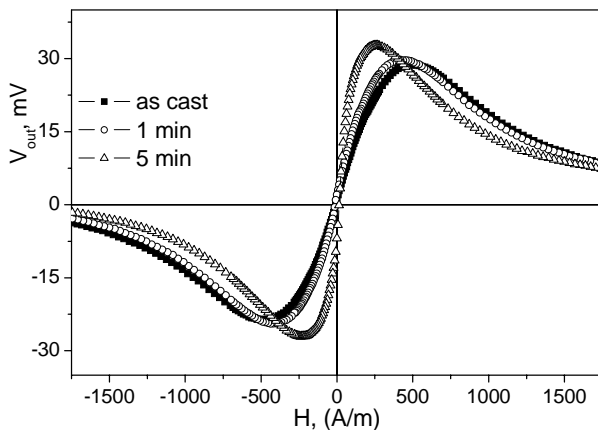


Fig. 7. $V_{out}(H)$ of Joule-heated $\text{Co}_{67}\text{Fe}_{3.85}\text{Ni}_{1.45}\text{B}_{11.5}\text{Si}_{14.5}\text{Mo}_{1.7}$ microwire annealed with 50 mA currents for different time.

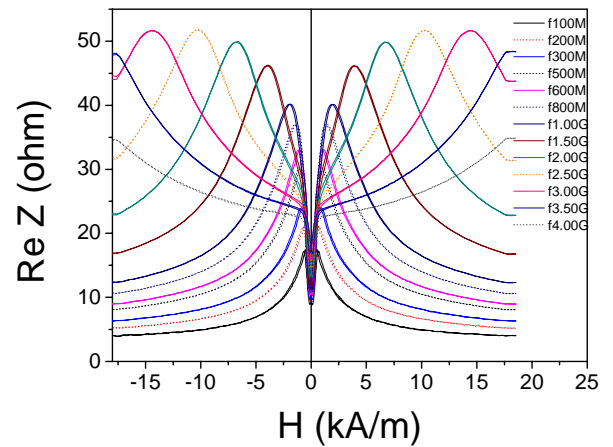


Fig. 8. $Z(H)$ dependence of $\text{Co}_{66}\text{Cr}_{3.5}\text{Fe}_{3.5}\text{B}_{16}\text{Si}_{11}$ microwires measured at different frequencies

It should be noted from Fig.6 that the $V_{out}(H)$ curves have asymmetrical shape exhibiting close to linear growth within the field range from $-H_m$ to H_m . The H_m limits the working range of MI sensor to 240 A/m and should be associated with the anisotropy field.

The influence of Joule heating on off-diagonal field characteristic of nearly zero-magnetostriction $\text{Co}_{67.1}\text{Fe}_{3.8}\text{Ni}_{1.4}\text{Si}_{14.5}\text{B}_{11.5}\text{Mo}_{1.7}$ microwire with diameters 9.4/17.0 μm is shown in Fig. 7. One can see that the thermal annealing with 50 mA DC current reduces the H_m from 480 A/m in as-cast state to 240 A/m after 5 min annealing. Thus, like in other families of magnetically soft amorphous wires [3, 22] magnetic anisotropy and GMI effect of glass-coated microwires can be tailored by heat treatments.

Recent applications and reduced dimensionality of developed microwires require extending frequency range for GMI studies and applications [21,23]. This particularly induced us to extend frequency range for GMI studies. Fig.8 presents results on magnetic field dependence of real part, Z' of the longitudinal wire impedance till 4 GHz. General features of these dependences is that the magnetic field of maximum shifts to the higher field region increasing the f .

3.4. GMI hysteresis in microwires with helical anisotropy

Another relevant feature is low field hysteresis that is observed in microwires with helical anisotropy even at high frequencies that can be observed in Fig.9.

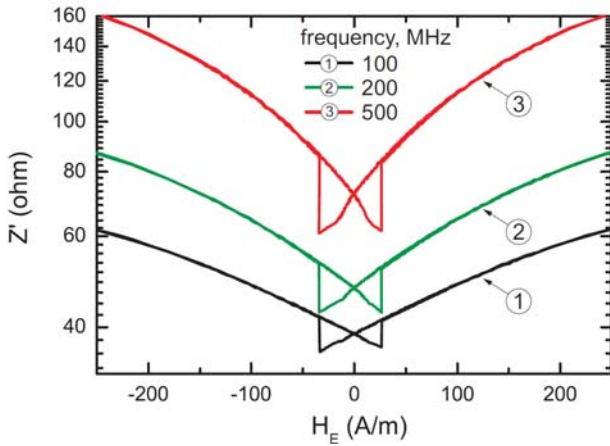


Fig. 9. Measured dependence $Z_{zz}(H_E)$ in $Co_{67.1}Fe_{3.8}Ni_{1.4}Si_{14.5}B_{11.5}Mo_{1.7}$ amorphous microwire with helical anisotropy. Experimental details are given in [11].

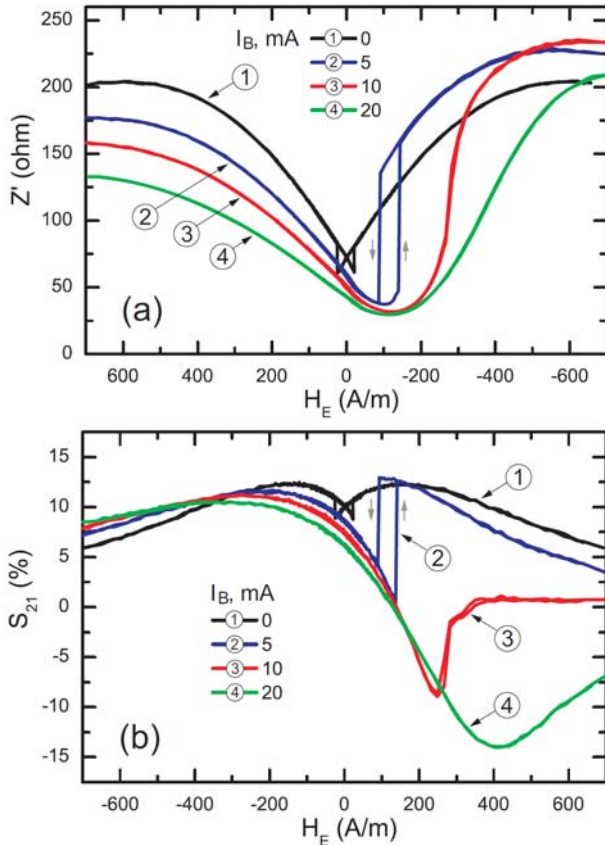


Fig. 10 Measured dependence longitudinal Z_{zz} (a) and off-diagonal impedance Z_{oz} (b) with a bias current I_B as parameter.

Recently we have developed a model for magnetization reversal and MI field dependence for nearly-zero-magnetostrictive amorphous microwires that demonstrates that low-field MI hysteresis arises from deviation of the anisotropy easy axis from transversal direction [11]. With the help of this model we were able to

obtain the main characteristics of the studied ferromagnetic microwire such as anisotropy field H_k and angle between the anisotropy easy axis and the transversal direction α . If the surface anisotropy is not circumferential, i.e. angle $\alpha \neq 0$, then the magnetization reversal process $\varphi_0(H_E)$ exhibits hysteresis and, consequently, the MI curve $Z(H_E)$ is also hysteretic. This hysteresis is usually undesirable for sensors application and can be suppressed by application of sufficiently high DC bias current I_B that creates a circumferential bias field $H_B > H_k \sin \alpha$. Fig.10 shows the experimental data of the bias current I_B effect on real part of longitudinal impedance of the wire Z' and the off-diagonal impedance Z_{oz} . As it seen, the MI curves at $I_B=0$ are symmetric and hysteretic. The application of $I_B=5$ mA results in braking the symmetry of both MI curves but the hysteresis is still present as the field H_B is not sufficiently high. When the I_B is increased to 10 mA, the inequality $H_B > H_k \sin \alpha$ is hold (previously we have found the parameters $H_k=265$ A/m, $\alpha = 35^\circ$ for this sample [14]) and MI curves becomes unhysteretic. Further increase of the bias current I_B results in the increasing of the field of impedance maximum and decreasing of the sensitivity (dZ/dH_E Slope) which is related to the effect of increasing magnetic hardness by bias field.

In fact, in practical application, a pulsed exciting scheme when the sharp pulses with pulse edge time about 5 ns are produced by passing square wave multi-vibrator pulses through the differentiating circuit is applied. Here the overall pulsed current contains a DC component I_B that produces bias circular magnetic field H_B [6, 21, 24]. In this way the hysteresis can be suppressed selecting adequate pulse amplitude.

As one can see, the application of I_B results in a shift of the minimum of MI curve and its rather high slope dZ/dH_E in the zero-field point. Also, a change of the bias current polarity results in mirroring of the MI curve. These finding can be used to develop of longitudinal MI sensor capable to detect both the magnitude and orientation of external field in extended field range beyond the anisotropy field H_k by the cross check on two MI curves taking with different I_B , for example $I_B = 10$ mA and $I_B = -20$ mA.

The condition of existence of examined effect is a helical magnetic anisotropy in the surface layer of the wire which origin should be attributed to complex internal stresses stored during simultaneous rapid solidification of metallic nucleus and glass coating [25]. In the case that the microwire in as-cast state possesses a circumferential anisotropy, the helical anisotropy can be induced by twisting the wire [14], moreover, the angle of helicoidality and, therefore, the resulting effect can be controlled by the degree of twisting.

Another interesting effect of MI in microwires with helical anisotropy is its sensitivity to dc bias current I_B . Usually, the MI is considered as the dependence of conductor impedance Z on an applied external magnetic field H_E . When a static bias current I_B is applied to the conductor, the MI dependence is defined also by this internal circumferential static bias field H_B . Recently we have demonstrated that that in a conductor with helical

magnetic anisotropy, the high frequency impedance depends on the dc bias current I_B (or the corresponding bias field H_B) and this dependence is hysteretic while the wire with circumferential anisotropy do not exhibit any sensitivity to the current I_B [26]. The physics of this effect is rather simple, it is associated with the fact that the current I_B creates the circumferential static magnetic field H_B which rotates the magnetization vector that result in the change of the impedance of the conductor. Fig.11 shows a set of dependences Z' on dc bias current I_B flowing through the wire with helical anisotropy at zero external magnetic field. As one can see, the impedance Z' is sensitive to the bias current I_B . Moreover, the dependence $Z'(I_B)$ is hysteretic and switching between high and low impedance states are observed.

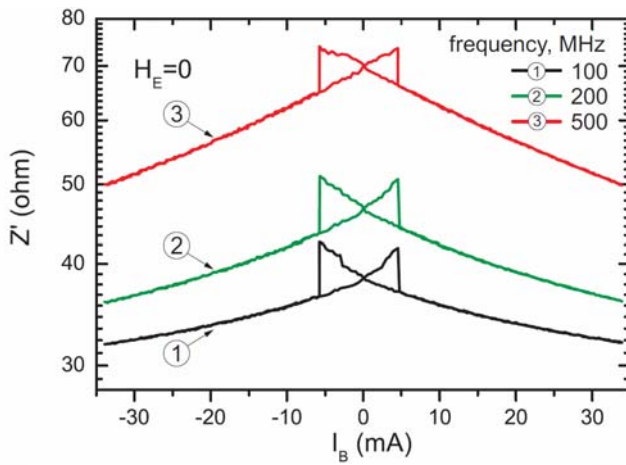


Fig 11 Experimental dependences of longitudinal impedance on bias current.

This effect of sensitivity of the wire impedance to the static current I_B can be used for different applications such as sensors of dc current. Similarly, as the effect depends on the anisotropy angle that can be used in stress or torque sensors; the impedance of the conductor will be sensitive to the applied torsional and tensile stresses. Also, as the impedance dependence is hysteretic, it can be used in memory elements. Further we consider the principle of operation of such memory element. Initially, independently on the initial state, after applying of a constant current pulse I_B in one direction (right to left in Fig 12a), the magnetic moments will orient along the easy axis in up direction (Fig. 12b) which corresponds to the store logical '1' state. Then, submitting the wire to external magnetic field makes the magnetic moments rotate in *close-to-circumferential* direction which characterized by low impedance (Fig. 12c) that can be easily detected. To write logical '0' one need to pass current pulse I_B in the opposite direction (left to right in d) that makes the magnetization orient along the easy axis in *down* direction (Fig 12e). In this case, the external magnetic field induces the magnetic moments rotation in *close-to-longitudinal* direction characterized by high impedance as shown in Fig. 12f. Similarly, to rotate the

magnetic moments from equi-impedance state (with the same impedance value), a small static current can be applied instead of external magnetic field H_E .

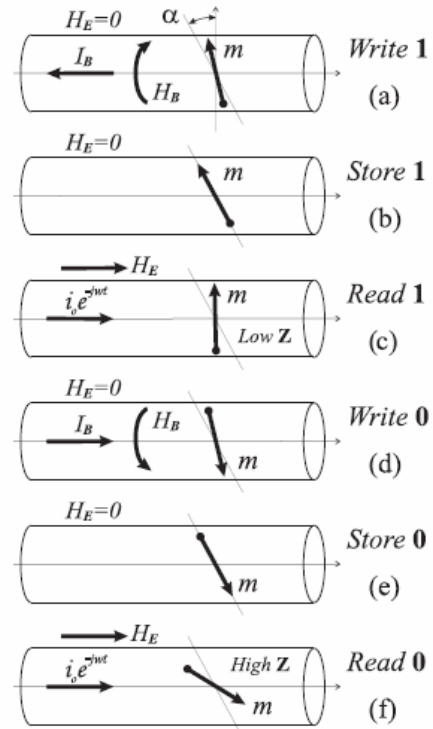


Fig.12 Applications of GMI hysteresis: Principle of data storage in wire element using MI hysteresis.

4. Conclusions

Thin amorphous wires with enhanced magnetic softness and GMI effect can be produced by the Taylor-Ulitovski technique. Magnetic properties and GMI effect of such microwires can be tailored by an appropriate selection of the metallic nucleus diameter, glass-coating thickness and chemical composition of the metallic nucleus and even by the heat treatment under magnetic field or without it. There are a number of interesting effects, such as induction of the transversal anisotropy in Fe-rich microwires allowing creating extremely stress sensitive elements. The investigation of diagonal and off-diagonal MI tensor component with pulse excitation in 6–12 μm amorphous glass-coated microwires has shown the grate potential of these materials for microminiaturized magnetic field sensor application. Their main advantages are high sensitivity low-hysteresis field dependence, low power consumption, and very simple sensor scheme are very promising for technological application. By varying the alloys composition and applying post fabrication processing it is possible to control the sensor's operating range. The off-diagonal impedance component in microwires with nearly zero magnetostriction is anti-symmetrical with close to linear behavior within the working range. The Joule heating of such microwires tends to

decreasing of magnetoelastic coupling and anisotropy field. Thermal treatment is an additional effective factor for tuning of MI dependence as well as the alloy composition and geometric parameters. Low field GMI hysteresis has been observed and explained in terms of helical magnetic anisotropy of microwires. The impedance of wire with helical anisotropy is sensitive to the bias field H_B . The hysteresis of impedance and switching between high and low impedance states was also observed. Data storage in MI microwire element using this hysteresis has been proposed.

Acknowledgments

The work was supported by the EU under project EM-safety, by ERA-NET program under Project "SoMaMicSens" (MANUNET-2010), by Spanish Ministry of Science and Innovation, MICINN, under Project MAT2010-18914 and by the Basque Government under 11 MIMAGURA project (S- PE11UN087). A. Zh. and V. Zh. wish to acknowledge the support of the Basque Government under Program of Mobility of the Investigating Personnel of the Department of Education, Universities and Investigation Grants MV-2009-2-21 and MV-2009-2-24.

References

- [1] DC Jiles Acta Materialia **51**, 5907 (2003).
- [2] V. Zhukova, M. Ipatov, A. Zhukov, Sensors **9**, 9216 (2009).
- [3] A. Zhukov, V. Zhukova, "Magnetic properties and applications of ferromagnetic microwires with amorphous and nanocrystalline structure", (New York: Nova Science Publishers, ISBN: 978-1-60741-770-5) (2009).
- [4] L. Panina, K. Mohri, Appl. Phys. Lett. **65**, 1189 (1994).
- [5] M.-H. Phan, H.-X. Peng, Progress in Materials Science **53**, 3232008
- [6] K. Mohri, T. Uchiyama, L. P. Shen, C. M. Cai, L. V. Panina, J. Magn. Magn. Mater. **249**, 351 (2002).
- [7] See <http://www.aichi-mi.com>.
- [8] A. Zhukov, M. Ipatov, J. Gonzalez, J.M. Blanco, V. Zhukova, J. Magn. Magn. Mater. **321**, 822 (2009).
- [9] V. Zhukova, A. Chizhik, A. Zhukov, A. Torcunov, V. Larin, J. Gonzalez, IEEE Trans Magn **38**, 3090 (2002).
- [10] S I Sandacci, D P. Makhnovskiy, L.V. Panina, K. Mohri, Y. Honkura, IEEE Trans Magn. **35**, 3505 (2004).
- [11] M. Ipatov, V. Zhukova, A. Zhukov, J. Gonzalez, A. Zvezdin, Phys. Rev. B **81**, 134421 (2010).
- [12] J. Velázquez, M. Vazquez, A. Zhukov, J Mater Res. **11**, 2499 (1996).
- [13] A. Antonov, I. Iakubov, A. Lagarkov, J. Magn. Magn. Mater., **187**, 252 (1998).
- [14] M. Ipatov, A. Chizhik, V. Zhukova, J. Gonzalez, A. Zhukov, J. Appl. Phys. **109**, 113924 (2011).
- [15] H. Chiriac, T. A. Ovari, Progress in Material Science **40**, 333 (1996).
- [16] A.S. Antonov, V.T. Borisov, O. V. Borisov, A.F. Prokoshin, N. A. Usov, J. Phys. D: Appl. Phys. **33**, 1161 (2000).
- [17] H. Fujimori, K.I. Arai, H. Shirae, H. Saito, T. Masumoto, N. Tsuya, Japan. J. Appl. Phys., **15**(4), 705 (1976).
- [18] A. Zhukov, J. Gonzalez, J.M. Blanco, M.J. Prieto, E. Pina, M. Vazquez, J. Appl. Phys. **87**, 1402 (2000).
- [19] A. Zhukov, Adv Func Mat **16**, 675 (2006).
- [20] A. Zhukov, C. Gómez-Polo, P. Crespo, M. Vázquez, J. Magn and Magn, Mater., **157/158**, 143-144 (1996).
- [21] K. Mohri, Y. Honkura Sensors letters, **5**, 267 (2007).
- [22] P. Ciureanu, G. Rudkowska, L. Clime, A. Sklyuyev, A. Yelon, J. Optoelectron. Adv. Mater. **6**, 905 (2004).
- [23] C. García, A. Zhukov, J. Gonzalez, V. Zhukova, J. M. Blanco, J. Optoelectron. Adv. Mater. **8**, 1706 (2006).
- [24] M. Ipatov, V. Zhukova, J. M. Blanco, J. Gonzalez, A. Zhukov, Phys. Stat. Sol. (a) **205**, 1779 (2008).
- [25] H. Chiriac, T.-A. Ovari, A. Zhukov, J. Magn. Magn. Mater., **254-255**, 469 (2003).
- [26] M. Ipatov, V. Zhukova, A. Zhukov, J. Gonzalez, Appl. Phys. Lett. **97**, 252507 (2010).

*Corresponding author: arkadi.joukov@ehu.es